



# Radiomics textural features by MR imaging to assess clinical outcomes following liver resection in colorectal liver metastases

Vincenza Granata<sup>1</sup> · Roberta Fusco<sup>2</sup> · Federica De Muzio<sup>3</sup> · Carmen Cutolo<sup>4</sup> · Sergio Venanzio Setola<sup>1</sup> · Roberta Grassi<sup>5</sup> · Francesca Grassi<sup>5</sup> · Alessandro Ottaiano<sup>6</sup> · Guglielmo Nasti<sup>6</sup> · Fabiana Tatangelo<sup>7</sup> · Vincenzo Pilone<sup>4</sup> · Vittorio Miele<sup>8,9</sup> · Maria Chiara Brunese<sup>3</sup> · Francesco Izzo<sup>10</sup> · Antonella Petrillo<sup>1</sup>

Received: 10 January 2022 / Accepted: 25 February 2022 / Published online: 26 March 2022  
© Italian Society of Medical Radiology 2022

## Abstract

**Purpose** To assess the efficacy of radiomics features obtained by T2-weighted sequences to predict clinical outcomes following liver resection in colorectal liver metastases patients.

**Methods** This retrospective analysis was approved by the local Ethical Committee board and radiological databases were interrogated, from January 2018 to May 2021, to select patients with liver metastases with pathological proof and MRI study in pre-surgical setting. The cohort of patients included a training set and an external validation set. The internal training set included 51 patients with 61 years of median age and 121 liver metastases. The validation cohort consisted a total of 30 patients with single lesion with 60 years of median age. For each volume of interest, 851 radiomics features were extracted as median values using PyRadiomics. Nonparametric test, intraclass correlation, receiver operating characteristic (ROC) analysis, linear regression modelling and pattern recognition methods (support vector machine (SVM), k-nearest neighbours (KNN), artificial neural network (NNET) and decision tree (DT)) were considered.

**Results** The best predictor to discriminate expansive versus infiltrative front of tumour growth was obtained by wavelet\_LHL\_gldm\_DependenceNonUniformityNormalized with an accuracy of 82%; to discriminate high grade versus low grade or absent was the wavelet\_LLH\_glcM\_Imc1 with accuracy of 88%; to differentiate the mucinous type of tumour was the wavelet\_LLH\_glcM\_JointEntropy with accuracy of 92% while to identify tumour recurrence was the wavelet\_LLL\_glcM\_Correlation with accuracy of 85%. Linear regression model increased the performance obtained with respect to the univariate analysis exclusively in the discrimination of expansive versus infiltrative front of tumour growth reaching an accuracy of 90%, a sensitivity of 95% and a specificity of 80%. Considering significant texture metrics tested with pattern recognition approaches, the best performance was reached by the KNN in the discrimination of the tumour budding considering the four textural predictors obtaining an accuracy of 93%, a sensitivity of 81% and a specificity of 97%.

**Conclusions** Ours results confirmed the capacity of radiomics to identify as biomarkers, several prognostic features that could affect the treatment choice in patients with liver metastases, in order to obtain a more personalized approach.

**Keywords** Liver metastasis · Magnetic resonance imaging · Radiomics · Pattern recognition · Outcome prediction

✉ Vincenza Granata  
r.fusco@igeamedical.com

<sup>1</sup> Division of Radiology, Istituto Nazionale Tumori IRCCS Fondazione Pascale – IRCCS di Napoli, Naples, Italy

<sup>2</sup> Medical Oncology Division, Igea SpA, Napoli, Italy

<sup>3</sup> Department of Medicine and Health Sciences “V. Tiberio”, University of Molise, 86100 Campobasso, Italy

<sup>4</sup> Department of Medicine, Surgery and Dentistry, University of Salerno, Salerno, Italy

<sup>5</sup> Division of Radiology, Università Degli Studi Della Campania Luigi Vanvitelli, Naples, Italy

<sup>6</sup> Division of Abdominal Oncology, Istituto Nazionale Tumori IRCCS Fondazione Pascale – IRCCS di Napoli, Naples, Italy

<sup>7</sup> Division of Pathology, Istituto Nazionale Tumori IRCCS Fondazione Pascale – IRCCS di Napoli, Naples, Italy

<sup>8</sup> Division of Radiology, Azienda Ospedaliera Universitaria Careggi, Florence, Italy

<sup>9</sup> Italian Society of Medical and Interventional Radiology (SIRM), SIRM Foundation, via della Signora 2, 20122 Milan, Italy

<sup>10</sup> Division of Epatobiliary Surgical Oncology, Istituto Nazionale Tumori IRCCS Fondazione Pascale – IRCCS di Napoli, Naples, Italy

## Introduction

Colorectal cancer (CRC) is one of the most habitually diagnosed tumour worldwide and metastatic disease is the main cause of death for patients with CRC. The liver is the most common site of distant metastases. A proper identification and characterization of liver lesions allows a better patients selection to avoid unnecessary treatment, so that the radiologist plays a crucial role in the multidisciplinary team of colorectal patients with liver metastases [1, 2]. Although computed tomography (CT) is usually the diagnostic method utilized for staging and surveillance, magnetic resonance imaging (MRI) is the main appreciated diagnostic tool in liver assessment thanks to its ability to provide morphological and functional data that improve the lesion characterization [1,2]. Radiomics is an encouraging field that explores medical images to acquire quantitative data that could be utilized as biomarkers to evaluate pathological processes at microscopic levels in order to increase diagnostic, prognostic and predictive accuracy in oncological setting [1–8]. The primary endo-point of radiomics is to improve the detection rate of tumours, which is accompanied by the need for a correct estimate of the prognosis and the identification of patients who are responsive to a specific treatment [9–14]. In this context, radiomic is conceived to be applied in decision support of precision medicine, using standard of care images that are routinely acquired in clinical practice, without burdening the costs of a radiological examination, both for patients and for health facilities [15–18]. Moreover, this tool, providing prognostic and/or predictive biomarker, offers a low-cost and repeatable instrument for longitudinal observing [19, 20].

Radiogenomics, that is the correlation of radiomics with patient molecular data, improves treatment, in the view of medicine adapted to the patient. Even if several studies have evaluated the radiogenomics in hepatocellular carcinoma, only few researches have assessed the radiomics in colorectal cancer liver metastases [1–3]. Imaging plays a crucial role in the management of patients with liver metastases having to guarantee not only an early diagnosis, but also a correct assessment post therapy, in order to avoid treatments that are harmful [21–24]. Although computed tomography (CT) is the diagnostic tool most often used during staging and follow-up, magnetic resonance imaging (MRI) is the only technique that allows to assess morphological and functional data of lesions, providing quantitative data that increase the characterization and the assessment after treatment [21–24].

In this setting, the opportunity to correlate radiomics data obtained by MRI to recurrence, mutational status, pathological characteristics (mucinous and tumour

budding) and surgical resection margin offers significant benefits with respect to qualitative assessment, allowing useful treatment selection in the perspective of personalized medicine. In the present study, we assessed the efficacy of radiomics features obtained by conventional T2-weighted (W) sequences-MRI to predict clinical outcomes following liver resection in colorectal liver metastases patients.

## Materials and methods

### Dataset characteristics

Local Ethical Committee board accepted this retrospective study renouncing to the patient consent signature for nature of the study.

Patient selection was made from January 2018 to May 2021 considering the following inclusion criteria: (1) liver pathological proven metastases; (2) MRI study of high quality in pre-surgical setting and (3) a follow-up CT scan of at least six months after surgery. The exclusion criteria were: (1) discordance among the imaging diagnosis and the pathologically ones, (2) no MRI studies. An external validation patient dataset was considered using data from “Careggi Hospital”, Florence, Italy. Therefore, the patient cohort included a training set and an external validation set. The internal training set included 51 patients (18 women and 33 men) with 61 years of median age (range 35–82 years) and 121 liver metastases. The external patient cohort consisted of 30 patients with single lesion (10 women and 20 men) with 60 years of median age (range 40–78 years).

As prognostic features we considered data obtained by pathological lesions assessment: (1) front of tumour growth: expansive versus infiltrative; (2) tumour budding: high grade versus low grade or absent; (3) mucinous type and clinical data obtained by follow-up; and 4) presence of recurrence.

The characteristics of the patients and their metastases are summarized in Table 1.

### MR imaging protocol and images post-processing

A Magnetom Symphony (Siemens, Erlangen, Germany) and Magnetom Aera (Siemens) equipped with an eight-element body and phased array coils were used to acquire MRI study protocol that includes breath-hold fat-saturated and not fat-saturated T2-weighted (T2-W) turbo spin-echo sequence, in- and opposed-phase T1-weighted (T1-W) gradient-echo sequence and fat-saturated (FS) T1-W gradient-echo sequence before and after contrast agent injection.

In this study, the radiomic features extraction was made considering the SPACE (sampling perfection with application-optimized contrasts using different flip angle evolution)

**Table 1** Characteristics of the study population (81 patients)

| Patient description            | Numbers (%) /range                 |
|--------------------------------|------------------------------------|
| Gender                         | Men 53 (65.4%)<br>Women 28 (34.6%) |
| Age                            | 61 y; range: 35–82 y               |
| Primary cancer site            |                                    |
| Colon                          | 52 (64.2%)                         |
| Rectum                         | 29 (35.8%)                         |
| Prior chemotherapy             | 81 (100%)                          |
| Hepatic metastases description |                                    |
| Patients with single nodule    | 52 (64.2%)                         |
| Patients with multiple nodules | 29 (35.8%) /range: 2–13 metastases |
| Nodule size (mm)               | Mean size 36.4 mm; range 7–58 mm   |
| Front of tumour growth         |                                    |
| Expansive                      | 30 (37.0%)                         |
| Infiltrative                   | 51 (63.0%)                         |
| Tumour budding                 |                                    |
| Absent                         | 12 (14.8%)                         |
| Low grade                      | 14 (17.3%)                         |
| High grade                     | 55 (67.9%)                         |
| Mucinous carcinoma             | 25 (30.9%)                         |
| Recurrence                     | 19 (23.5%)                         |
| RAS mutation                   | 42 (51.9%)                         |

fat suppressed sequences. Detailed data regarding the MR imaging parameters are summarized in Table 2.

Regions of interest (ROIs) were manually drawn slice-by-slice on SPACE images by two expert radiologists with 22 and 15 years of abdominal imaging experience, first separately and then together and in accordance with each other. Radiomics features were extracted as median values by the volumes of interest obtained by the consensus of two radiologists. No registration techniques to decrease movements artefacts were applied; however, the use of median value of metrics reduce the influence by artefacts.

The ROIs definition was made using segmentation tool of 3DSlicer [<https://www.slicer.org/>].

Radiomic Features were extracted using PyRadiomics [<https://pyradiomics.readthedocs.io/en/latest/features.html>] that includes First Order Statistics (19 features); Shape-based (3D) (16 features); Shape-based (2D) (10 features); Gray Level Cooccurrence Matrix (24 features); Gray Level Run Length Matrix (16 features); Gray Level Size Zone Matrix (16 features); Neighbouring Gray Tone Difference Matrix (5 features); Gray Level Dependence Matrix (14 features).

The features are calculated according to the definitions of the Imaging Biomarker Standardization Initiative (IBSI). Details about radiomics features are reported in [<https://readthedocs.org/projects/pyradiomics/downloads/>] [22, 25].

### Statistical analysis

Univariate and multivariate analysis were performed using the Statistics and Machine Learning Toolbox of MATLAB R2021b (MathWorks, Natick, MA, USA).

The assessment of observer variability was made calculating the intraclass correlation coefficient. The nonparametric Kruskal–Wallis test was performed to identify differences statistically significant among clinical parameters and radiomic metrics of two groups (front of tumour growth: expansive versus infiltrative; tumour budding: high grade versus low grade or absent; mucinous type; and presence of recurrence).

Receiver operating characteristic (ROC) analysis was made and the Youden index was used to individuate the optimal cut-off value for each feature and area under the ROC curve (AUC), sensitivity, positive predictive value (PPV), negative predictive value (NPV) and accuracy. McNemar test was used to demonstrate difference statistically significant in the performance results of dichotomy tables. A *p* value < 0.05 was considered as significant for each statistical test.

**Table 2** MR Sequence parameters

| Sequence          | Orientation | TR/TE/FA (ms/ms/deg.) | AT (min) | Acquisition matrix | ST/Gap (mm) | FS                       |
|-------------------|-------------|-----------------------|----------|--------------------|-------------|--------------------------|
| Trufisp T2-W      | Coronal     | 4.30/2.15/80          | 0.46     | 512×512            | 4 / 0       | Without                  |
| HASTE T2-W        | Axial       | 1500/90/170           | 0.36     | 320×320            | 5 / 0       | Without and with (SPAIR) |
| HASTE T2w         | Coronal     | 1500/92/170           | 0.38     | 320×320            | 5 / 0       | Without                  |
| SPACE T2W FS      | Axial       | 4471/259/120          | 4.20     | 384×450            | 3/0         | With (SPAIR)             |
| In–Out phase T1-W | Axial       | 160/2.35/70           | 0.33     | 256×192            | 5 / 0       | Without                  |
| Vibe T1-W         | Axial       | 4.80/1.76/12          | 0.18     | 320×260            | 3 / 0       | With (SPAIR)             |

TR = Repetition time, TE = Echo time, FA = Flip angle, AT = Acquisition time, ST = Slice thickness, FS = Fat suppression, SPAIR = Spectral adiabatic inversion recovery, HASTE = Half Fourier single-shot turbo spin-echo, SPACE = Sampling perfection with application-optimized contrasts using different flip angle evolution

To identify the combinations of variables with the best results in the prediction of the clinical outcomes, a multivariate analysis was performed. Clinical outcome considered were: (1) front of tumour growth: expansive versus infiltrative; (2) tumour budding: high grade versus low grade or absent; (3) mucinous type; and (4) presence of recurrence.

A first selection of variables was made based on the results obtained from the univariate analysis considering only the features that at univariate analysis had an accuracy superior a threshold reported in Table 3.

A linear regression modelling was used to assess the best linear model of textural features considered as predictors for each outcome. ROC analysis with Youden index was used to identify the optimal cut-off value of the linear model and to obtain sensitivity, specificity, PPV and NPV.

Moreover, pattern recognition methods include support vector machine (SVM), k-nearest neighbours (KNN), artificial neural network (NNET), and decision tree (DT). The best model was chosen considering the highest area under ROC curve and highest accuracy. A 10-k fold cross validation approach was used to individuate the best classifier on the training set while the external validation cohort was used to validate the findings of the best classifier.

## Results

The median value of intraclass correlation coefficients for features was 0.91 (range 0.86–0.95).

Among significant features to differentiate the front of tumour growth, 15 textural parameters obtained an accuracy  $\geq 70\%$  (Table 4). The best performance to discriminate expansive versus infiltrative front of tumour growth was obtained by wavelet\_LHL\_gldm\_DependenceNonUniformityNormalized with accuracy of 82%, a sensitivity of 99%, a specificity of 53% and a PPV and a NPV of 78% and 96%, respectively, with a cut-off value of 0.06.

Among significant features to differentiate the tumour budding, four textural parameters obtained an accuracy  $\geq 85\%$  (Table 4). The best performance to discriminate high grade versus low grade or absent was the wavelet\_LLH\_glcml\_Imc1 with accuracy of 88%, a sensitivity of 93%, a specificity of 71% and a PPV and a NPV of 90% and 79%, respectively, with a cut-off value of -0.14.

Among significant features to differentiate the mucinous type of tumour, 15 textural parameters obtained an accuracy  $\geq 87\%$  (Table 4). The best performance to differentiate the mucinous type of tumour was obtained by the wavelet\_LLH\_glcml\_JointEntropy with accuracy of 92%, a sensitivity of 83%, a specificity of 94% and a PPV and a NPV of 78% and 95%, respectively, with a cut-off value of 4.61.

**Table 3** (Sub)datasets, variables selection criteria and predictors combinations

|           | Outcome variable       | Predictors used in multivariate analysis | Accuracy threshold on univariate analysis in order to perform a feature selection |
|-----------|------------------------|--|---|
| Dataset 1 | Front of tumour growth | 15 radiomic metrics                      | $\geq 0.70$   |
| Dataset 2 | Tumour budding         | 4 radiomic metrics                       | $\geq 0.85$   |
| Dataset 3 | Mucinous type          | 15 radiomic metrics                      | $\geq 0.87$   |
| Dataset 4 | Recurrence presence    | 6 radiomic metrics                       | $\geq 0.80$   |

**Table 4** Findings by univariate analysis with ROC performance results

| The best predictors at Univariate analysis | Respect to tumour growth front                     | Respect to tumour budding | Respect to mucinous type       | Respect to recurrences        |
|--|--|---------------------------|--------------------------------|-------------------------------|
|  | Wavelet_LHL_gldm_DependenceNonUniformityNormalized | Wavelet_LLH_glcml_Imc1    | Wavelet_LLH_glcml_JointEntropy | Wavelet_LLL_glcml_Correlation |
| AUC  | 0.67   | 0.77                      | 0.85                           | 0.63                          |
| Sensitivity                                | 0.99   | 0.93                      | 0.83                           | 0.52                          |
| Specificity                                | 0.53   | 0.71                      | 0.94                           | 0.97                          |
| PPV  | 0.78   | 0.90                      | 0.78                           | 0.84                          |
| NPV  | 0.96   | 0.79                      | 0.95                           | 0.85                          |
| Accuracy                                   | <b>0.82</b>  | <b>0.88</b>               | <b>0.92</b>                    | <b>0.85</b>                   |
| Cut-off                                    | 0.06   | -0.14                     | 4.61                           | 0.88                          |

Among significant features to identify tumour recurrence, six textural parameters obtained an accuracy  $\geq 80\%$  (Table 4). The best performance to identify tumour recurrence was obtained by the wavelet\_LLL\_glcm\_Correlation with accuracy of 85%, a sensitivity of 52%, a specificity of 97% and a PPV and a NPV of 84% and 85%, respectively, with a cut-off value of 0.88.

Linear regression model increased the performance obtained with respect to the univariate analysis exclusively in the discrimination of expansive versus infiltrative front of tumour growth while for the other predictions the univariate analysis obtained the highest accuracy (see Tables 5 and 6, Fig. 1). In the discrimination of the of expansive versus infiltrative front of tumour growth the linear model of the 15 predictors reached an accuracy of 90%, a sensitivity of 95%, a specificity of 80% and a PPV 89% and NPV of 90%, respectively.

Considering significant texture metrics tested with pattern recognition approaches, the best performance for the identification of the front of tumour growth was reached by a decision tree while for the discrimination of tumour budding, mucinous type and presence of recurrence by a KNN (Table 5, Fig. 2). The best accuracy was reached by the KNN

in the discrimination of the tumour budding considering the four textural predictors (original\_glcm\_Idn; wavelet\_HLL\_glcm\_InverseVariance; wavelet\_LHL\_gldm\_DependenceNonUniformityNormalized; wavelet\_LLH\_glcm\_Imc1): (AUC of 0.93; an accuracy of 93%; sensitivity of 81%; and a specificity of 97%).

Significant difference in terms of accuracy among univariate and multivariate analysis was obtained only in the prediction of tumour growth front both considering linear model and the decision tree and in the prediction of tumour budding considering the KNN compared to the accuracy obtained by the single best predictor at the univariate analysis (p value <0.05 at McNemar test).

### Discussion and Conclusions

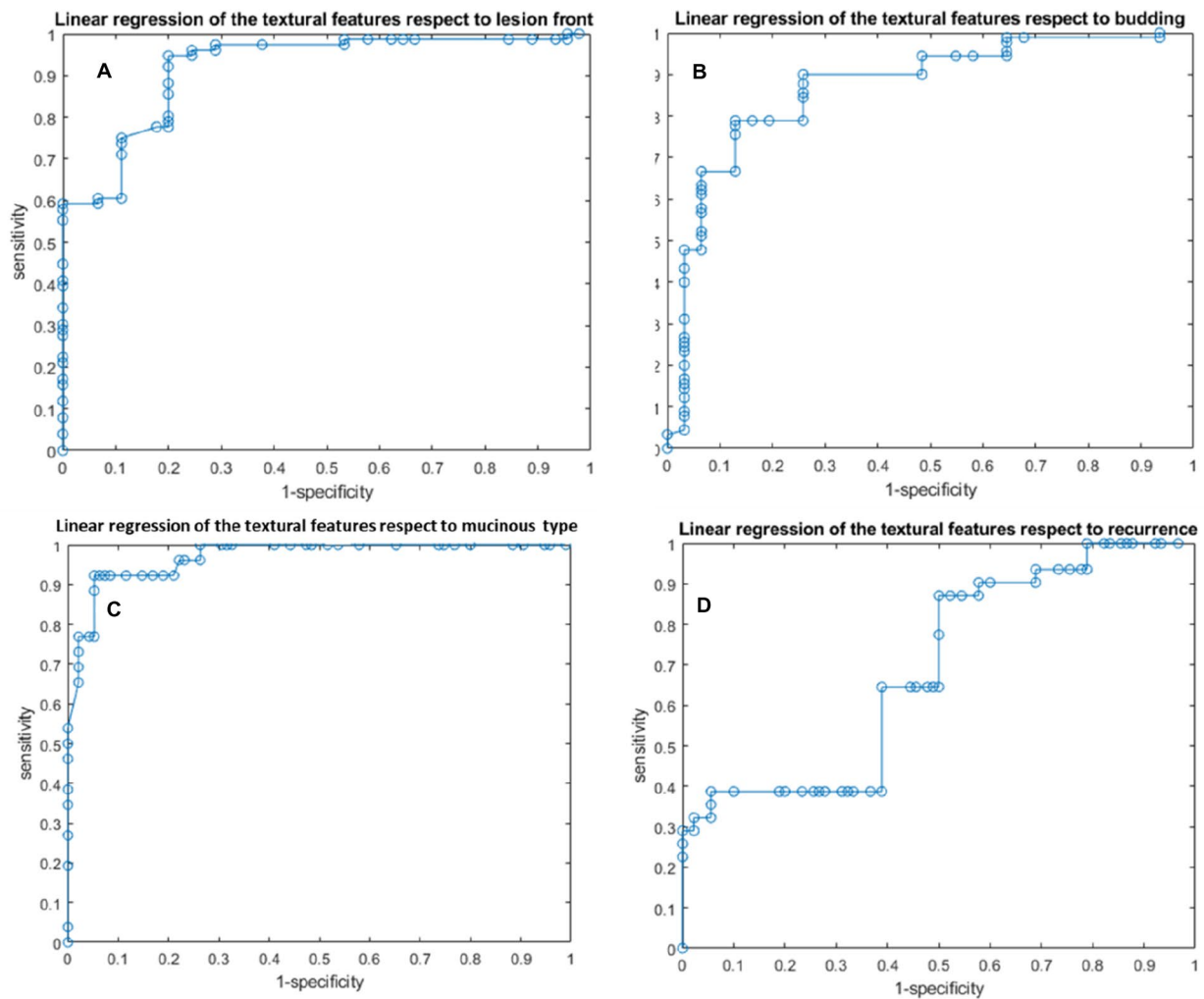
The present study demonstrated that radiomics analysis can be identified as biomarkers, several features that could impact on the therapeutic choice in colorectal liver metastases patients. Our data were verified by external validation dataset.

**Table 5** Linear regression and pattern recognition analysis with significant features

| Linear regression with predictors identified at univariate analysis            | AUC            | Sensitivity | Specificity | PPV         | NPV         | Accuracy            | Cut-off  |
|--|----------------|-------------|-------------|-------------|-------------|---------------------|--|
| Linear model respect to the tumour growth front                                | 0.90           | 0.95        | 0.80        | 0.89        | 0.90        | 0.90                | 1.51   |
| Linear model respect to the tumour budding                                     | 0.80           | 0.79        | 0.87        | 0.95        | 0.59        | 0.81                | 0.73   |
| Linear model respect to the mucinous type                                      | 0.96           | 0.92        | 0.95        | 0.83        | 0.98        | 0.94                | 0.26   |
| Linear model respect to the recurrence presence                                | 0.66           | 0.87        | 0.50        | 0.38        | 0.92        | 0.60                | 0.18   |
| Pattern recognition analysis with predictors identified at univariate analysis | Dataset        | AUC         | Accuracy    | Sensitivity | Specificity | Training time [sec] | Settings of model  |
| Decision tree  | Training set   | 0.9         | 89.3        | 84          | 92          | 11.1                | Fine Tree; Maximum number of splits:100; split criterion: Gini's diversity index; optimizer options: Hyperparameter options disabled |
|  | Validation set | 0.88        | 86.1        | 86          | 86          |                     |  |
| KNN  | Training set   | 0.93        | 92.6        | 81          | 97          | 8.9                 | Weighted KNN; number of neighbours:10; distance metric: Euclidean; distance weight: squared inverse                                  |
|  | Validation set | 0.86        | 91.7        | 67          | 100         |                     |  |
|  | Training set   | 0.92        | 89.3        | 96          | 65          | 3.2                 |  |
|  | Validation set | 0.83        | 88.9        | 93          | 71          |                     |  |
|  | Training set   | 0.84        | 90.1        | 95          | 73          | 2.5                 |  |
|  | Validation set | 0.9         | 91.7        | 93          | 87          |                     |  |

**Table 6** Linear regression model parameters with respect to the tumour growth front

| Features   | Coefficients | P value |
|--|--------------|---------|
| Intercept  | − 10.99      | 0.01    |
| Original_shape_SurfaceVolumeRatio                  | − 1.13       | 0.24    |
| Wavelet_HLL_gldm_InverseVariance                   | 13.96        | 0.01    |
| Wavelet_HLL_firstorder_Median                      | 0.14         | 0.06    |
| Wavelet_HLL_gldm_ShortRunEmphasis                  | 38.72        | 0.00    |
| Wavelet_HLL_gldm_RunPercentage                     | − 38.39      | 0.00    |
| Wavelet_LHL_gldm_DependenceNonUniformityNormalized | − 7.33       | 0.61    |
| Wavelet_LHL_gldm_InverseVariance                   | − 3.19       | 0.51    |
| Wavelet_LHL_firstorder_Kurtosis                    | 0.01         | 0.04    |
| Wavelet_LHL_gldm_ShortRunEmphasis                  | − 24.29      | 0.21    |
| Wavelet_LHL_gldm_RunPercentage                     | 46.40        | 0.00    |
| Wavelet_LHL_gldm_RunLengthNonUniformityNormalized  | − 14.58      | 0.15    |
| Wavelet_LLH_gldm_Imc1                              | − 0.31       | 0.87    |
| Wavelet_LLL_firstorder_Uniformity                  | 6.76         | 0.17    |
| Wavelet_LLL_firstorder_Minimum                     | 0.01         | 0.00    |
| Wavelet_LLL_gldm_GrayLevelNonUniformityNormalized  | − 5.61       | 0.28    |

**Fig. 1** ROC curves of linear regression analysis respect to the tumour growth front (A), the tumour budding (B), the tumour mucinous type (C) and the recurrence presence (D)

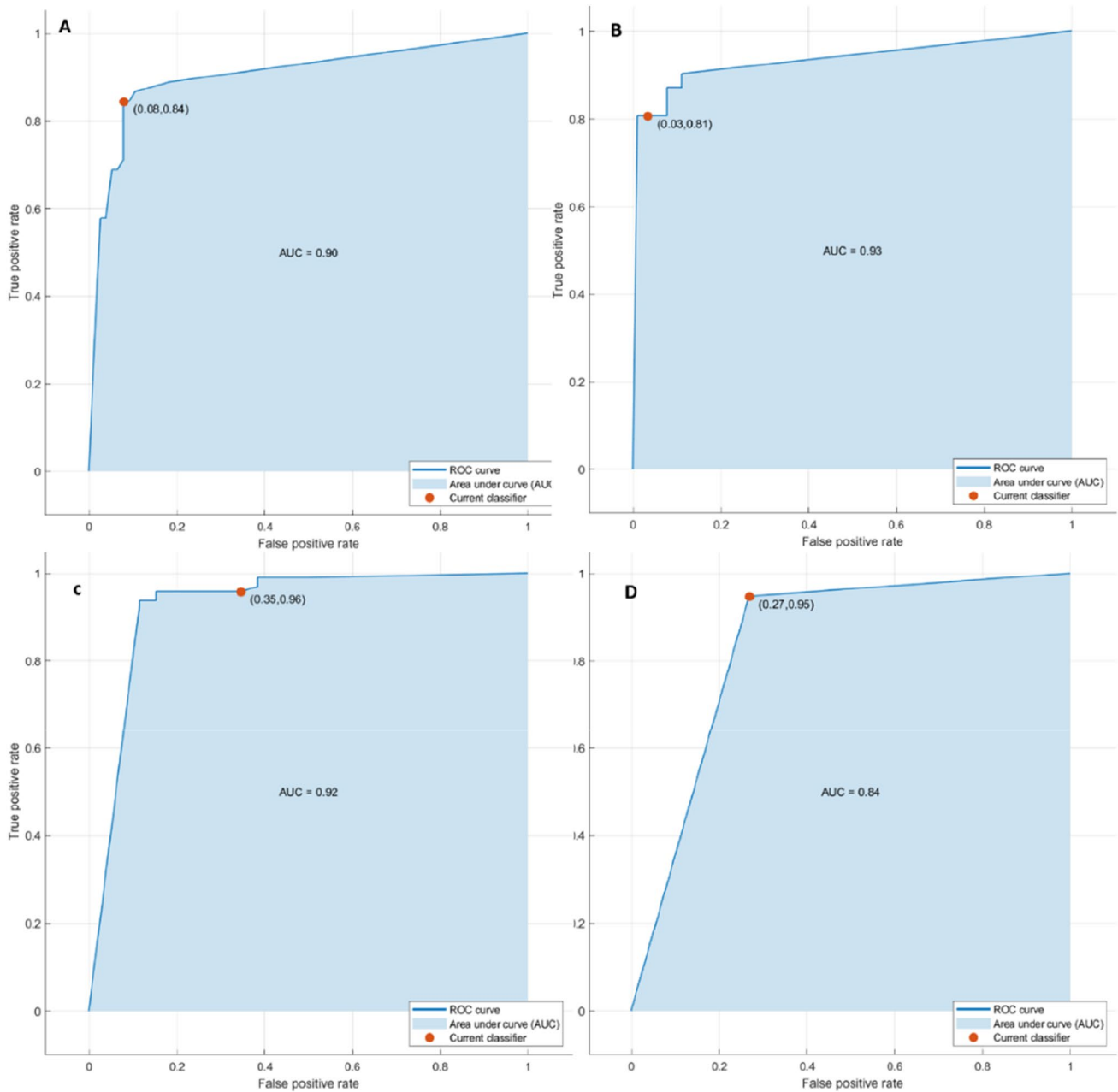


**Fig. 2** ROC curves of the best classifier respect to the tumour growth front (A), the tumour budding (B), the tumour mucinous type (C) and the recurrence presence (D)

We obtained a good performance considering the single textural significant metric in the identification of front of tumour growth (expansive versus infiltrative) and tumour budding (high grade versus low grade or absent), in the recognition of mucinous type and in the detection of recurrences.

With regard to the front of tumour growth, 15 textural parameters obtained an accuracy  $\geq 70\%$  and the best performance was obtained by wavelet\_LHL\_gldm\_DependenceNonUniformityNormalized with accuracy of 82%, a

sensitivity of 99%, a specificity of 53% and a PPV and a NPV of 78% and 96%, respectively, with a cut-off value of 0.06.

Regarding tumour budding, four textural parameters obtained an accuracy  $\geq 85\%$  and the best performance to discriminate high grade versus low grade or absent was the wavelet\_LLH\_gldm\_Imc1 with accuracy of 88%, a sensitivity of 93%, a specificity of 71% and a PPV and a NPV of 90% and 79%, respectively, with a cut-off value of  $-0.14$ .

Among significant features to differentiate the mucinous type of tumour, 15 textural parameters obtained an accuracy  $\geq 87\%$ . The best performance was obtained by the wavelet\_LLH\_glm\_JointEntropy with accuracy of 92%, a sensitivity of 83%, a specificity of 94% and a PPV and a NPV of 78% and 95%, respectively, with a cut-off value of 4.61.

With regard to tumour recurrence, six textural parameters obtained an accuracy  $\geq 80\%$ . The best performance was obtained by the wavelet\_LLL\_glm\_Correlation with accuracy of 85%, a sensitivity of 52%, a specificity of 97% and a PPV and a NPV of 84% and 85%, respectively, with a cut-off value of 0.88.

Linear regression model increased the performance obtained with respect to the univariate analysis exclusively in the discrimination of expansive versus infiltrative front of tumour growth while for the other predictions the univariate analysis obtained the highest accuracy.

Several studies demonstrated the correlation between radiomics parameters and prognosis [26–39]. An association between homogeneity and worse overall survival (OS) was demonstrated by Andersen et al. [31]. According to Rahmim et al. radiomic parameters of heterogeneity obtained by FDG PET were predictors of lower OS [36]. Lubner et al. demonstrated that the degree of skewness was inversely correlated to KRAS while the entropy was related to OS [33]. In addition to the survival advantages, the possibility to predict recurrence in liver has been demonstrated [36–39]. According to our results, Ravanelli et al. related high CT uniformity and low OS and PFS in patients with CRC and liver metastasis [38].

Radiomics and radiogenomics are emerging tools with significant limits. The major limit is the heterogeneity of software employed in different studies, so as the variety of imaging devices in different clinics. This evidently hampers the reading of different results in multicentre studies. In addition, the segmentation could affect the results [39–47].

The present study has several limitations: (1) the small population analysed, although the investigation was done on a homogeneous sample and on individual lesion; (2) the retrospective nature of the study; (3) a manual segmentation, that, although several researches support automatic segmentation to avoid inter-observer variability, in our opinion, the manual approach is more realistic. Moreover, we not assessed the impact of the different sequences as T1-W or diffusion weighted imaging so as the different phases of contrast study. Data that we plan to evaluate in a future study are shown in Table 6.

Ours results confirmed the capacity of radiomics to identify as biomarkers, several prognostic features that could affect the treatment choice in patients with liver metastases, in order to obtain a more personalized approach. These results were confirmed by external

validation dataset. We obtained a good performance considering the single textural significant metric in the identification of front of tumour growth (expansive versus infiltrative) and tumour budding (high grade versus low grade or absent), in the identification of mucinous type and in the detection of recurrences.

**Acknowledgements** The authors are grateful to Alessandra Trocino, librarian at the National Cancer Institute of Naples, Italy. Moreover, for the collaboration, authors are grateful for the research support to Paolo Pariate, Martina Totaro and Andrea Esposito of Radiology Division, “Istituto Nazionale Tumori IRCCS Fondazione Pascale – IRCCS di Napoli”, Naples, I-80131, Italy

**Funding** The authors have not disclosed any funding.

**Data Availability** Data are available at the link <https://zenodo.org/record/6374234#.YjjY3erMK3A>.

## Declarations

**Conflict of interest** No conflicts of interest.

**Research involving human participants and/or animals** The research was conducted in accordance with the principles embodied in the Declaration of Helsinki and in accordance with local statutory requirements.

**Informed consent** Local Ethical Committee board accepted this retrospective study renouncing to the patient consent signature for nature of the study.

## References

1. Granata V, Fusco R, Avallone A, De Stefano A, Ottaiano A, Sbordone C, Brunese L, Izzo F, Petrillo A (2021) Radiomics-Derived Data by Contrast Enhanced Magnetic Resonance in RAS Mutations Detection in Colorectal Liver Metastases. *Cancers (Basel)* 25;13(3):453. doi: <https://doi.org/10.3390/cancers13030453>.
2. Granata V, Fusco R, Risi C, Ottaiano A, Avallone A, De Stefano A, Grimm R, Grassi R, Brunese L, Izzo F, Petrillo A (2020) Diffusion-Weighted MRI and Diffusion Kurtosis Imaging to Detect RAS Mutation in Colorectal Liver Metastasis. *Cancers (Basel)* 26;12(9):2420. doi: <https://doi.org/10.3390/cancers12092420>.
3. Granata V, Fusco R, Barretta ML, Picone C, Avallone A, Belli A, Patrone R, Ferrante M, Cozzi D, Grassi R, Grassi R, Izzo F, Petrillo A (2021) Radiomics in hepatic metastasis by colorectal cancer. *Infect Agent Cancer* 2;16(1):39. doi: <https://doi.org/10.1186/s13027-021-00379-y>.
4. Granata V, Fusco R, Costa M, Picone C, Cozzi D, Moroni C, La Casella GV, Montanino A, Monti R, Mazzoni F, Grassi R, Malagano VG, Cappabianca S, Grassi R, Miele V, Petrillo A (2021). Preliminary Report on Computed Tomography Radiomics Features as Biomarkers to Immunotherapy Selection in Lung Adenocarcinoma Patients. *Cancers (Basel)* 7;13(16):3992. doi: <https://doi.org/10.3390/cancers13163992>. Fusco R, Piccirillo A, Sansone M, Granata V, Rubulotta MR, Petrosino T, Barretta ML, Vallone P, Di Giacomo R, Esposito E, Di Bonito M, Petrillo A (2021) Radiomics and Artificial Intelligence Analysis with Textural Metrics Extracted by Contrast-Enhanced Mammography in the



- Breast Lesions Classification. *Diagnostics* (Basel) 30;11(5):815. doi: <https://doi.org/10.3390/diagnostics11050815>.
5. Fusco R, Granata V, Mazzei MA, Meglio ND, Roscio DD, Moroni C, Monti R, Cappabianca C, Picone C, Neri E, Coppola F, Montanino A, Grassi R, Petrillo A, Miele V (2021) Quantitative imaging decision support (QIDS™) tool consistency evaluation and radiomic analysis by means of 594 metrics in lung carcinoma on chest CT scan. *Cancer Control* 28:1073274820985786. <https://doi.org/10.1177/1073274820985786> PetraliaG, SummersPE, AgostiniA, AmbrosiniR, CianciR, CristelG, CalistriL, ColagrandeS (2020) Dynamiccontrast-enhancedMRIinoncology:howwedoit. *RadiolMed* 125,1288–1300, <https://doi.org/10.1007/s11547-020-01220-z>
  6. Ria F, Samei E (2020) Is regulatory compliance enough to ensure excellence in medicine? *Radiol Med* 125:904–905. <https://doi.org/10.1007/s11547-020-01171-5>
  7. Zhang A, Song J, Ma Z, Chen T (2020) Combined dynamic contrast-enhanced magnetic resonance imaging and diffusion-weighted imaging to predict neoadjuvant chemotherapy effect in FIGO stage IB2-IIA2 cervical cancers. *Radiol Med* 125:1233–1242. <https://doi.org/10.1007/s11547-020-01214-x>
  8. Crimi F, Capelli G, Spolverato G, Bao QR, Florio A, Milite Rossi S, Cecchin D, Albertoni L, Campi C, Pucciarelli S, Stramare R (2020) MRI T2-weighted sequences-based texture analysis (TA) as a predictor of response to neoadjuvant chemo-radiotherapy (nCRT) in patients with locally advanced rectal cancer (LARC). *Radiol Med* 125:1216–1224. <https://doi.org/10.1007/s11547-020-01215-w>
  9. Kirienko M, Ninatti G, Cozzi L, Voulaz E, Gennaro N, Barajon I, Ricci F, Carlo-Stella C, Zucali P, Sollini M, Balzarini L, Chiti A (2020) Computed tomography (CT)-derived radiomic features differentiate prevascular mediastinum masses as thymic neoplasms versus lymphomas. *Radiol Med* 125:951–960. <https://doi.org/10.1007/s11547-020-01188-w>
  10. Zhang L, Kang L, Li G, Zhang X, Ren J, Shi Z, Li J, Yu S (2020) Computed tomography-based radiomics model for discriminating the risk stratification of gastrointestinal stromal tumors. *Radiol Med* 125:465–473. <https://doi.org/10.1007/s11547-020-01138-6>
  11. Gurgitano M, Angileri SA, Rodà GM, Liguori A, Pandolfi M, Ierardi AM, Wood BJ, Carrafiello G (2021) Interventional Radiology ex-machina: impact of Artificial Intelligence on practice. *Radiol Med* 126(7):998–1006. <https://doi.org/10.1007/s11547-021-01351-x>
  12. Scapicchio C, Gabelloni M, Barucci A, Cioni D, Saba L, Neri E (2021) A deep look into radiomics. *Radiol Med* 126(10):1296–1311. <https://doi.org/10.1007/s11547-021-01389-x>
  13. Wei J, Jiang H, Gu D, Niu M, Fu F, Han Y, Song B, Tian J (2020) Radiomics in liver diseases: Current progress and future opportunities. *Liver Int Sep*;40(9):2050–2063. doi: <https://doi.org/10.1111/liv.14555>.
  14. Saini A, Breen I, Pershad Y, Naidu S, Knuttinen MG, Alzubaidi S, Sheth R, Albadawi H, Kuo M, Oklu R. Radiogenomics and Radiomics in Liver Cancers (2018) *Diagnostics* (Basel) 27;9(1):4. doi: <https://doi.org/10.3390/diagnostics9010004>.
  15. de la Pinta C, Castillo ME, Collado M, Galindo-Pumariño C, Peña C (2021) Radiogenomics: Hunting Down Liver Metastasis in Colorectal Cancer Patients. *Cancers* (Basel) 5;13(21):5547. doi: <https://doi.org/10.3390/cancers13215547>.
  16. Nardone V, Reginelli A, Grassi R, Boldrini L, Vacca G, D'Ippolito E, Annunziata S, Farchione A, Belfiore MP, Desideri I, Cappabianca S (2021) Delta radiomics: a systematic review. *Radiol Med* 126(12):1571–1583. <https://doi.org/10.1007/s11547-021-01436-7>
  17. Brunese L, Brunese MC, Carbone M, Ciccone V, Mercaldo F, Santone A (2021) Automatic PI-RADS assignment by means of formal methods. *Radiol Med*. <https://doi.org/10.1007/s11547-021-01431-y>
  18. van der Lubbe MFJA, Vaidyanathan A, de Wit M, van den Burg EL, Postma AA, Brintjes TD, Bilderbeek-Beckers MAL, Dammeijer PFM, Bossche SV, Van Rompaey V, Lambin P, van Hoof M, van de Berg R (2021) A non-invasive, automated diagnosis of Menière's disease using radiomics and machine learning on conventional magnetic resonance imaging: A multicentric, case-controlled feasibility study. *Radiol Med*. <https://doi.org/10.1007/s11547-021-01425-w>
  19. Granata V, Fusco R, Avallone A, Cassata A, Palaia R, Delrio P, Grassi R, Tatangelo F, Grazzini G, Izzo F, Petrillo A (2020) Abbreviated MRI protocol for colorectal liver metastases: How the radiologist could work in pre surgical setting. *PLoS One* 15;15(11):e0241431. doi: <https://doi.org/10.1371/journal.pone.0241431>.
  20. Granata V, Fusco R, Venanzio Setola S, Mattace Raso M, Avallone A, De Stefano A, Nasti G, Palaia R, Delrio P, Petrillo A, Izzo F (2019) Liver radiologic findings of chemotherapy-induced toxicity in liver colorectal metastases patients. *Eur Rev Med Pharmacol Sci* 23(22):9697–9706. [https://doi.org/10.26355/eurev\\_201911\\_19531](https://doi.org/10.26355/eurev_201911_19531)
  21. Granata V, Fusco R, Maio F, Avallone A, Nasti G, Palaia R, Albino V, Grassi R, Izzo F, Petrillo A (2019) Qualitative assessment of EOB-GD-DTPA and Gd-BT-DO3A MR contrast studies in HCC patients and colorectal liver metastases. *Infect Agent Cancer* 27(14):40. <https://doi.org/10.1186/s13027-019-0264-3>
  22. Granata V, Fusco R, de Lutio di Castelguidone E, Avallone A, Palaia R, Delrio P, Tatangelo F, Botti G, Grassi R, Izzo F, Petrillo A, (2019) Diagnostic performance of gadoteric acid-enhanced liver MRI versus multidetector CT in the assessment of colorectal liver metastases compared to hepatic resection. *BMC Gastroenterol* 19(1):129. <https://doi.org/10.1186/s12876-019-1036-7>
  23. <https://pyradiomics.readthedocs.io/en/latest/features.html>
  24. Zwanenburg A, Vallières M, Abdalah MA, Aerts HJWL, Andrearczyk V, Apte A, Ashrafinia S, Bakas S, Beukinga RJ, Boellaard R, Bogowicz M, Boldrini L, Buvat I, Cook GJR, Davatzikos C, Depeursinge A, Desserot MC, Dinapoli N, Dinh CV, Echegaray S, El Naqa I, Fedorov AY, Gatta R, Gillies RJ, Goh V, Götz M, Guckenberger M, Ha SM, Hatt M, Isensee F, Lambin P, Leger S, Leijenaar RTH, Lenkowitz J, Lippert F, Losnegård A, Maier-Hein KH, Morin O, Müller H, Napel S, Nioche C, Orhac F, Pati S, Pfahler EAG, Rahmim A, Rao AUK, Scherer J, Siddique MM, Sijtsma NM, Socarras Fernandez J, Spezi E, Steenbakkers RJHM, Tanadini-Lang S, Thorwarth D, Troost EGC, Upadhyaya T, Valentini V, van Dijk LV, van Griethuysen J, van Velden FHP, Whybra P, Richter C, Lööck S (2020) The Image Biomarker Standardization Initiative: Standardized Quantitative Radiomics for High-Throughput Image-based Phenotyping. *Radiology* 295:328–338. <https://doi.org/10.1148/radiol.2020191145>
  25. Granata V, Fusco R, Avallone A, Catalano O, Piccirillo M, Palaia R, Nasti G, Petrillo A, Izzo F (2018) A radiologist's point of view in the presurgical and intraoperative setting of colorectal liver metastases. *Future Oncol* 14(21):2189–2206. <https://doi.org/10.2217/fon-2018-0080>
  26. Granata V, Fusco R, Catalano O, Avallone A, Palaia R, Botti G, Tatangelo F, Granata F, Cascella M, Izzo F, Petrillo A (2017) Diagnostic accuracy of magnetic resonance, computed tomography and contrast enhanced ultrasound in radiological multimodality assessment of peribiliary liver metastases. *PLoS ONE* 12(6):e0179951. <https://doi.org/10.1371/journal.pone.0179951>
  27. Granata V, Fusco R, Catalano O, Filice S, Amato DM, Nasti G, Avallone A, Izzo F, Petrillo A (2015) Early Assessment of Colorectal Cancer Patients with Liver Metastases Treated with Antiangiogenic Drugs: The Role of Intravoxel Incoherent Motion

- in Diffusion-Weighted Imaging. *PLoS ONE* 10(11):e0142876. <https://doi.org/10.1371/journal.pone.0142876>
28. Beckers RCJ, Trebeschi S, Maas M, Schnerr RS, Sijmons JML, Beets GL, Houwers JB, Beets-Tan RGH, Lambregts DMJ (2018) CT texture analysis in colorectal liver metastases and the surrounding liver parenchyma and its potential as an imaging biomarker of disease aggressiveness, response and survival. *Eur J Radiol* 102:15–21. <https://doi.org/10.1016/j.ejrad.2018.02.031>
  29. Andersen IR, Thorup K, Andersen MB, Olesen R, Mortensen FV, Nielsen DT, Rasmussen F (2019) Texture in the monitoring of regorafenib therapy in patients with colorectal liver metastases. *Acta Radiol* 60(9):1084–1093. <https://doi.org/10.1177/0284185118817940>
  30. Zhang H, Li W, Hu F, Sun Y, Hu T, Tong T (2019) MR texture analysis: potential imaging biomarker for predicting the chemotherapeutic response of patients with colorectal liver metastases. *Abdom Radiol (NY)* 44(1):65–71. <https://doi.org/10.1007/s00261-018-1682-1>
  31. Lubner MG, Stabo N, Lubner SJ, del Rio AM, Song C, Halberg RB, Pickhardt PJ (2015) CT textural analysis of hepatic metastatic colorectal cancer: pre-treatment tumor heterogeneity correlates with pathology and clinical outcomes. *Abdom Imaging* 40(7):2331–2337. <https://doi.org/10.1007/s00261-015-0438-4>
  32. Simpson AL, Doussot A, Creasy JM, Adams LB, Allen PJ, DeMatteo RP, Gönen M, Kemeny NE, Kingham TP, Shia J, Jarnagin WR, Do RKG, D'Angelica MI (2017) Computed Tomography Image Texture: A Noninvasive Prognostic Marker of Hepatic Recurrence After Hepatectomy for Metastatic Colorectal Cancer. *Ann Surg Oncol* 24(9):2482–2490. <https://doi.org/10.1245/s10434-017-5896-1>
  33. Ganeshan B, Miles KA, Young RC, Chatwin CR. Hepatic enhancement in colorectal cancer: texture analysis correlates with hepatic hemodynamics and patient survival (2007) *Acad Radiol* 14(12):1520–30. doi: <https://doi.org/10.1016/j.acra.2007.06.028>.
  34. Rahmim A, Bak-Fredslund KP, Ashrafinia S, Lu L, Schmidtlein CR, Subramaniam RM, Morsing A, Keiding S, Horsager J, Munk OL (2019) Prognostic modeling for patients with colorectal liver metastases incorporating FDG PET radiomic features. *Eur J Radiol* 113:101–109. <https://doi.org/10.1016/j.ejrad.2019.02.006>
  35. Dercle L, Lu L, Schwartz LH, Qian M, Tejpar S, Eggleton P, Zhao B, Piessevaux H (2020) Radiomics Response Signature for Identification of Metastatic Colorectal Cancer Sensitive to Therapies Targeting EGFR Pathway. *J Natl Cancer Inst* 112:902–912. <https://doi.org/10.1093/jnci/djaa017>
  36. Ravanelli M, Agazzi GM, Tononcelli E, Roca E, Cabassa P, Baiocchi G, Berruti A, Maroldi R (2019) Farina D (2019) Texture features of colorectal liver metastases on pretreatment contrast-enhanced CT may predict response and prognosis in patients treated with bevacizumab-containing chemotherapy: a pilot study including comparison with standard chemotherapy. *Radiol Med* 124(9):877–886. <https://doi.org/10.1007/s11547-019-01046-4>
  37. Taghavi M, Staal FC, Simões R, Hong EK, Lambregts DM, van der Heide UA, Beets-Tan RG, Maas M (2021) CT radiomics models are unable to predict new liver metastasis after successful thermal ablation of colorectal liver metastases. *Acta Radiol* 17:2841851211060437. <https://doi.org/10.1177/02841851211060437>
  38. Rizzetto F, Calderoni F, De Mattia C, Defeudis A, Giannini V, Mazzetti S, Vassallo L, Ghezzi S, Sartore-Bianchi A, Marsoni S, Siena S, Regge D, Torresin A, Vanzulli A (2020) Impact of inter-reader contouring variability on textural radiomics of colorectal liver metastases. *Eur. Radiol. Exp* 10;4(1):62. doi: <https://doi.org/10.1186/s41747-020-00189-8>.
  39. Coppola F, Giannini V, Gabelloni M, Panic J, Defeudis A, Lo Monaco S, Cattabriga A, Cocozza MA, Pastore LV, Polici M, Caruso D, Laghi A, Regge D, Neri E, Golfieri R, Faggioni L (2021) Radiomics and Magnetic Resonance Imaging of Rectal Cancer: From Engineering to Clinical Practice. *Diagnostics (Basel)* 11(5):756. <https://doi.org/10.3390/diagnostics11050756>
  40. Esposito A, Buscarino V, Raciti D, Casiraghi E, Manini M, Biondetti P, Forzenigo L (2020) Characterization of liver nodules in patients with chronic liver disease by MRI: performance of the Liver Imaging Reporting and Data System (LI-RADS vol 2018) scale and its comparison with the Likert scale. *Radiol Med* 125(1):15–23. <https://doi.org/10.1007/s11547-019-01092-y>
  41. Bozkurt M, Eldem G, Bozbulut UB, Bozkurt MF, Kılıçkap S, Peynircioğlu B, Çil B, Lay Ergün E, Volkan-Salanci B (2021) Factors affecting the response to Y-90 microsphere therapy in the cholangiocarcinoma patients. *Radiol Med* 126(2):323–333. <https://doi.org/10.1007/s11547-020-01240-9>
  42. Granata V, Grassi R, Fusco R, Setola SV, Belli A, Ottaiano A, Nasti G, La Porta M, Danti G, Cappabianca S, Cutolo C, Petrillo A (2021) Izzo F (2021) Intrahepatic cholangiocarcinoma and its differential diagnosis at MRI: how radiologist should assess MR features. *Radiol Med* 126(12):1584–1600. <https://doi.org/10.1007/s11547-021-01428-7>
  43. Cusumano D, Meijer G, Lenkiewicz J, Chiloiro G, Boldrini L, Masciocchi C, Dinapoli N, Gatta R, Casà C, Damiani A, Barbaro B, Gambacorta MA, Azario L, De Spirito M, Intven M, Valentini V (2021) A field strength independent MR radiomics model to predict pathological complete response in locally advanced rectal cancer. *Radiol Med* 126(3):421–429. <https://doi.org/10.1007/s11547-020-01266-z>
  44. Bertocchi E, Barugola G, Nicosia L, Mazzola R, Ricchetti F, Dell'Abate P, Alongi F, Ruffo G (2020) A comparative analysis between radiation dose intensification and conventional fractionation in neoadjuvant locally advanced rectal cancer: a monocentric prospective observational study. *Radiol Med* 125:990–998. <https://doi.org/10.1007/s11547-020-01189-9>
  45. Fornell-Perez R, Vivas-Escalona V, Aranda-Sanchez J, Gonzalez-Dominguez MC, Rubio-Garcia J, Aleman-Flores P, Lozano-Rodriguez A, Porcel-de-Peralta G, Loro-Ferrer JF (2020) Primary and post-chemoradiotherapy MRI detection of extramural venous invasion in rectal cancer: the role of diffusion-weighted imaging. *Radiol Med* 125(6):522–530. <https://doi.org/10.1007/s11547-020-01189-9>
  46. Schicchi N, Fogante M, Palumbo P, Agliata G, Esposto Pirani P, Di Cesare E, Giovagnoni A (2020) The sub-millisievert era in CTCA: the technical basis of the new radiation dose approach. *Radiol Med* 125(11):1024020–01137–7.
  47. Park SH, Kim YS, Choi J. Dosimetric analysis of the effects of a temporary tissue expander on the radiotherapy technique. *Radiol Med* 126(3):437–444. doi: <https://doi.org/10.1007/s11547-020-01297-6>.

**Publisher's Note** Springer Nature remains neutral with regard to jurisdictional claims in published maps and institutional affiliations.